

Proceedings of SPIE-The International Society for Optical Engineering

**Application of
Optical Instrumentation
in Medicine IX**

March 22-24, 1981

Proceedings of SPIE—The International Society for Optical Engineering

Volume 273

Application of Optical Instrumentation in Medicine IX

Joel E. Gray, Arthur G. Haus, William S. Properzio, James A. Mulvaney
Editors

March 22-24, 1981
San Francisco, California

Published by
SPIE—The International Society for Optical Engineering
P.O. Box 10, Bellingham, Washington 98227 U.S.A.
206/676-3290

The papers appearing in this book comprise the proceedings of the meeting mentioned on the cover and title page. They reflect the authors' opinions and have not been reviewed, refereed, edited, or copyedited by SPIE. Their inclusion in this publication does not necessarily constitute endorsement by the editors or by SPIE—The International Society for Optical Engineering.

Please use the following format to cite material from this book:

Author(s), "Title of Paper," *Application of optical instrumentation in medicine IX*, Proc. Soc. Photo-Opt. Instr. Eng. 273, page numbers (1981).

Library of Congress Catalog Card No.: 74-169214

ISBN 0-89252-305-0

© 1981 by the Society of Photo-Optical Instrumentation Engineers, 405 Fieldston Road, Bellingham, Washington 98227 USA. All rights reserved. No part of this book may be reprinted, or reproduced or utilized in any form or by any electronic, mechanical, or other means, now known or hereafter invented, including photo-copying and recording, or in any information storage or retrieval system, without permission in writing from the publisher.

Printed in the United States of America.

APPLICATION OF OPTICAL INSTRUMENTATION IN MEDICINE IX

Volume 273

Program Committee

Chairman

Joel E. Gray

Mayo Clinic

Co-Chairmen

Arthur G. Haus

University of Texas System Cancer Center

William S. Properzio

Bureau of Radiological Health, FDA

James A. Mulvaney

University of Colorado Health Sciences Center

Chairman Session 1—Special Session—Nuclear Magnetic Resonance Imaging: Current Status

C. Leon Partain

Vanderbilt University

Co-Moderator

A. Everette James, Jr.

Vanderbilt University

Chairman Session 2—Conventional Imaging Systems Evaluation

Arthur G. Haus

University of Texas System Cancer Center

Chairman Session 3—Digital Radiography

William S. Properzio

Bureau of Radiological Health, FDA

Chairman Session 4—Quality Control

James A. Mulvaney

University of Colorado Health Sciences Center

Chairman Session 5—Nuclear Medicine

Joel E. Gray

Mayo Clinic

Break-Out Session A—Nuclear Magnetic Resonance

C. Leon Partain

Vanderbilt University

Break-Out Session B—Computerized Tomography

Gary D. Fullerton

University of Texas Health Sciences Center, San Antonio

Break-Out Session C—Digital Imaging

William S. Properzio

Bureau of Radiological Health, FDA

Break-Out Session D—Conventional Imaging Systems Evaluation

Joel E. Gray

Mayo Clinic

Chairmen Session 6—Joint Session with the American Roentgen Ray Society

Arthur G. Haus

University of Texas System Cancer Center

James F. Martin

Bowman-Gray School of Medicine

Chairman Session 7—Computerized Tomography

Gary D. Fullerton

University of Texas Health Sciences Center, San Antonio

Chairman Session 8—Recording, Storage, and Processing of Images

Joel E. Gray

Mayo Clinic

APPLICATION OF OPTICAL INSTRUMENTATION IN MEDICINE IX

Volume 273

INTRODUCTION

During the past few years, there has been a dramatic change in medical imaging subsequent to the introduction of new diagnostic imaging modalities and techniques. Computerized tomography and ultrasonography have found their place in the field of diagnostic radiology. Conventional radiography has become more complex due to many factors, including the availability of new intensifying screens such as rare earth screens, new developments in image intensifier and fluoroscopic systems, specially sensitized lower silver content films, chemistry and film processor advances, x-ray tube target materials, selective beam filtration, x-ray tube focal spot size considerations for reducing geometric unsharpness and for magnification techniques, carbon fiber and low absorbing materials for cassettes and table tops, and scatter reducing techniques such as scanning multiple slit methods. Test procedures for quality assurance and equipment compliance are becoming increasingly more important in the radiology department. Advances in nuclear medicine imaging have taken place, in particular, computer-assisted cardiac studies and emission tomography. At present, digital radiographic techniques and nuclear magnetic resonance (NMR) are being used or considered as diagnostic imaging methods. With such an increase in possibilities, important decisions must be made in order to select the best diagnostic imaging modality, system or technique for the appropriate diagnostic task. These decisions will be based on three fundamental considerations: (1) diagnostic information and accuracy; (2) patient risk (radiation dose); and (3) monetary costs.

The SPIE Application of Optical Instrumentation in Medicine scientific programs and resulting proceedings publications have provided valuable information on the topics outlined above. In recent years, this meeting has been presented jointly by the Society of Photo-Optical Instrumentation Engineers (SPIE) (now SPIE—The International Society for Optical Engineering) and the Society of Photographic Scientists and Engineers (SPSE) and has been held in conjunction with the American Roentgen Ray Society (ARRS) meeting. The meeting has been held in cooperation with the Bureau of Radiological Health, the American Roentgen Ray Society, the American Association of Physicists in Medicine, and the Society for Radiological Engineering. The program has provided a format for important scientific contributions to both the clinical and technical aspects of conventional and new imaging systems, techniques and methods of evaluation.

The 1981 Application of Optical Instrumentation in Medicine IX meeting was held in March in San Francisco, CA. Nearly 300 physicians, physicists, and engineers

from medical institutions and industry were registered. Invited and contributed papers were presented in eight sessions. The session topics were: (1) nuclear magnetic resonance (NMR); (2) conventional imaging systems evaluation; (3) digital radiography; (4) quality control; (5) nuclear medicine; (6) joint session with the ARRS; (7) computerized tomography; and (8) recording, storage and processing of images. The joint session with invited or specially selected papers from the Application of Optical Instrumentation in Medicine IX and the ARRS meetings produced an overflow turnout. Much of the interest for this year's meeting was in digital radiography and NMR imaging. Separate break-out sessions on NMR, computerized tomography, digital imaging and conventional imaging system evaluation provided for lively informal discussions.

Arthur G. Haus
M.D. Anderson Hospital & Tumor Institute
University of Texas System Cancer Center

APPLICATION OF OPTICAL INSTRUMENTATION IN MEDICINE IX

Volume 273

Contents

Program Committee	viii
Introduction	x
SESSION 1. SPECIAL SESSION—NUCLEAR MAGNETIC RESONANCE IMAGING: CURRENT STATUS	
273-01 Nuclear magnetic resonance (NMR) tomography at Nottingham: methods system technology and results	1 2
G. N. Holland, W. S. Moore, R. C. Hawkes, University of Nottingham, United Kingdom	
273-02 Nuclear magnetic resonance (NMR) imaging at Hammersmith Hospital	8
J. C. Gore, F. H. Doyle, J. M. Pennock, Hammersmith Hospital, United Kingdom	
273-04 Nuclear magnetic resonance (NMR) imaging at the University of California, San Francisco	11
Lawrence E. Crooks, Robert Herfkens, Peter L. Davis, University of California, San Francisco	
273-05 Phosphorus nuclear magnetic resonance (NMR) of myocardial infarction using surface coils	16
Ray L. Nunnally, The University of Texas Health Science Center at Dallas	
273-06 Three-dimensional display of nuclear magnetic resonance images	35
Gabor T. Herman, Jayaram K. Udupa, State University of New York at Buffalo; David M. Kramer, Paul C. Lauterbur, State University of New York at Stony Brook; Andrew M. Rudin, Northport Veterans Administration Medical Center; Jay S. Schneider, State University of New York at Stony Brook	
273-07 A whole body nuclear magnetic resonance (NMR) imaging system with full three-dimensional capabilities	41
Howard E. Simon, State University of New York at Stony Brook	
SESSION 2. CONVENTIONAL IMAGING SYSTEMS EVALUATION	
273-08 Exposure limits imposed by screen-film systems on the transfer of image information	51 52
J. W. Motz, C. E. Dick, M. Danos, National Bureau of Standards	
273-09 Influence of ambient light on the "visual" sensitometric properties of, and detail perception on, a radiograph	57
Romain Bollen, Jean Vranckx, Agfa-Gevaert N.V., Belgium	
273-10 Sensitometry at low x-ray energies	63
Daniel R. Bednarek, Stephen Rudin, Roland Wong, State University of New York at Buffalo	

273-11	Screen speed designations: a need for standardization and some suggestions	67
	Gilbert Zweig, Arkwright Incorporated	
273-12	Variation with kVp of exposure and attenuation throughout a radiographic system and assessment of the speed of films, screens, and processors	73
	Cupido Daniels, Kenneth W. Taylor, University of Toronto, Canada	
273-13	X-ray phantom development for observer performance studies	77
	C. A. Kelsey, R. D. Moseley, F. A. Mettler, T. W. Parker, University of New Mexico School of Medicine	
273-14	Quantification of silver in radiographic film	80
	Martin J. Yaffe, Gordon E. Mawdsley, Ontario Cancer Institute, Canada	
SESSION 3. DIGITAL RADIOGRAPHY		87
273-15	Performance characteristics of a digital fluorographic system	88
	S. J. Riederer, F. A. DiBianca, J-P J. Georges, G. A. Jensen, G. S. Keyes, N. J. Pelc, E. R. Steinike, W. H. Wesbey, General Electric Medical Systems	
273-16	An understanding of digital radiography through image computer simulation	96
	Jean-Pierre J. Georges, Gary S. Keyes, Norbert J. Pelc, Stephen J. Riederer, General Electric Medical Systems Division	
273-17	Digital radiography: spatial and contrast resolution	103
	Paul Bjorkholm, M. Annis, E. Frederick, J. Stein, R. Swift, American Science and Engineering, Inc.	
273-18	Characteristics of a linear xenon detector array for digital radiography	108
	D. J. Drost, A. Fenster, University of Toronto, Canada	
273-19	Digital radiography using the Quantex DS-20	114
	G. Allan Johnson, K. Ford, R. Heinz, Duke University Medical Center	
273-20	Evaluation of renal function by digital subtraction imaging	120
	O. Nalcioğlu, J. A. Seibert, W. W. Roeck, R. M. Friedenbergl, H. Rosenberg, University of California; J. G. Pearce, University of Southern California; J. L. Gehrich, American Edwards Laboratory	
273-21	Digital subtraction fluoroscopic system with tandem video processing units	125
	Robert G. Gould, Martin J. Lipton, University of California; Paul Mengers, Roger Dahlberg, Quantex, Corporation	
SESSION 4. QUALITY CONTROL		133
273-22	Phantoms of the accurate simulation of energy-dependent patient/x-ray beam interactions	134
	Robert J. Jennings, Bureau of Radiological Health	
273-23	Computer controlled technique factors in diagnostic radiology	137
	Bhas K. Pillai, University of California at San Francisco; Robert G. Waggener, William D. McDavid, The University of Texas Health Science Center at San Antonio	
273-24	Determination of x-ray tube potential (kV) waveform by a noninvasive evaluation of radiation output (NERO)	149
	William E. Simon, Doug Richards, Victoreen, Inc.	

273-25	System-level performance testing of image-intensified x-ray equipment	153
	James A. Mulvaney, Raymond P. Rossi, James T. Spicka, University of Colorado Health Sciences Center	
273-26	Performance evaluation of image intensifiers coupled with photofluorographic camera and their clinical application	160
	Pei-Jan Paul Lin, Harvey L. Neiman, Richard A. Mintzer, Sheridan N. Meyers, Northwestern Memorial Hospital	
273-27	Photographic method for measurement of image intensifier tube contrast	168
	Robert J. Moore, Loma Linda University Medical Center	
273-28	Evaluation of the resolution limit for radiological procedures	177
	Arthur G. Haus, Jeffrey Meyer, Deborah K. Guebert, The University of Texas System Cancer Center	
SESSION 5. NUCLEAR MEDICINE		187
273-29	Tube by tube analysis of field uniformity for gamma cameras	188
	G. Donald Frey, Armand P. Glassman, Medical University of South Carolina	
273-31	Computer simulation of image reconstruction with a new electronically collimated gamma tomography system	192
	M. Singh, D. Doria, University of Southern California	
273-32	Computer generated cardiac model for nuclear medicine	201
	John F. Hills, Tom R. Miller, The Edward Mallinckrodt Institute of Radiology	
BREAK-OUT SESSION A. NUCLEAR MAGNETIC RESONANCE		207
BREAK-OUT SESSION B. COMPUTERIZED TOMOGRAPHY		207
BREAK-OUT SESSION C. DIGITAL IMAGING		207
BREAK-OUT SESSION D. CONVENTIONAL IMAGING SYSTEMS EVALUATION		207
SESSION 6. JOINT SESSION WITH THE AMERICAN ROENTGEN RAY SOCIETY		209
273-34	Potential hazards in nuclear magnetic resonance (NMR) imaging: heating effects of changing magnetic fields and rf fields on small metallic implants	210
	Peter Davis, Lawrence Crooks, Mitsuaki Arakawa, Robert McRee, Leon Kaufman, Alexander R. Margulis, University of California	
273-35	Digital radiography: an overview	215
	Ben A. Arnold, Harvey Eisenberg, David Borger, Alexander Methereil, South Bay Hospital	
273-36	Photoelectronic digital radiology: development and evaluation leading to intravenous angiography	227
	H. D. Fisher, S. Nudelman, T. W. Ovitt, M. P. Capp, M. M. Frost, D. Ouimette, H. Roehrig, Arizona Health Sciences Center	
273-38	Efficient use of silver halide in x-ray film	232
	R. E. Wayrynen, E. I. du Pont de Nemours & Company, Inc.	
273-39	Anatomy of silver recovery	235
	Donald E. Titus, Eastman Kodak Company	

273-40	Dual-kVp radiography	239
	William R. Brody, Graham Sommer, Leonard A. Lehmann, Albert Macovski, Robert E. Alvarez, Stanford University; Norbert J. Pelc, Stephen J. Riederer, Anne Hall, General Electric Company	
273-41	X-ray microbeam system with a discrete-spot target	244
	Osamu Fujimura, Bell Laboratories; Marvin E. Haskin, Hahnemann Medical College and Hospital	

SESSION 7. COMPUTERIZED TOMOGRAPHY255

273-42	Fundamentals of computerized tomography (CT) tissue characterization of the brain	256
	Gary D. Fullerton, Ernesto Blanco, University of Texas Health Science Center at San Antonio	
273-43	Tissue characterization with contrast enhancement of the brain	267
	D. B. Plewes, M. Violante, University of Rochester Medical Center	
273-44	Tissue characterization by dynamic contrast enhancement of the brain	278
	Leon Axel, University of California, San Francisco	
273-45	Computerized heavy-ion tomography	283
	W. R. Holley, C. A. Tobias, J. I. Fabrikant, J. Llacer, W. T. Chu, E. V. Benton, Lawrence Berkeley Laboratory	
273-46	Split-filter computed tomography (CT) for routine dual energy scanning	294
	Brian Rutt, Aaron Fenster, University of Toronto, Ontario, Canada	
273-47	Tissue characterization using energy-selective computed tomography	301
	Robert E. Alvarez, William H. Marshall, Roger Lewis, Stanford University	
273-48	Dependence of the computerized tomography (CT) number—electron density relationship on patient size and x-ray beam filtration for fan beam CT scanners	308
	M. E. Masterson, C. L. Thomason, R. McGary, M. A. Hunt, L. D. Simpson, D. W. Miller, J. S. Laughlin, Memorial Sloan-Kettering Cancer Center	
273-49	Evaluation of multiplanar imaging capabilities of four current computed tomography (CT) scanners	318
	G. Allan Johnson, Melvyn Korobkin, E. Ralph Heinz, Duke University Medical Center	
273-50	Sampling the Radon transformation in conventional computed tomography	326
	Dennis L. Parker, Vernon Smith, Kristian R. Peschmann, John L. Couch, University of California at San Francisco	

SESSION 8. RECORDING, STORAGE, AND PROCESSING OF IMAGES337

273-52	Design of a multiformat camera for medical fluoroscopy	338
	Ernest W. Edmonds, Mohawk College, Ontario, Canada; David M. Hynes, Dennis Baranoski, John Rowlands, St. Joseph's Health Centre, Toronto, Canada; Karl R. Krametz, Siemens Electric Company, Toronto, Canada	

273-52	Video-photographic system for rapid inexpensive unit-record recording and flexible replay of real-time ultrasonic imaging of the breast	343
	Bayard Gardineer, Charles Howlett, Sidney Krieger, Gerard Lazzaro, David Lyons, Reuben Mezrich, Donald Wiseman, Special Research Group of Technicare	
273-53	Reducing patient exposure and operating room procedure time with electronic imaging	348
	Gerald R. Edelstein, Albert Einstein Medical Center	
273-54	Digital processing of conventional tomograms	350
	Michael W. Vannier, R. Gilbert Jost, Washington University School of Medicine	
273-55	Digital storage compression for diagnostic images	357
	M. J. Flynn, J. S. Newman, R. M. Mares, The Mt. Sinai Hospital of Cleveland	
Author Index		369
Subject Index		370

APPLICATION OF OPTICAL INSTRUMENTATION IN MEDICINE IX

Volume 273

SESSION 1

SPECIAL SESSION—NUCLEAR MAGNETIC RESONANCE IMAGING: CURRENT STATUS

Session Chairman

C. Leon Partain

Vanderbilt University

Co-Moderator

A. Everette James, Jr.

Vanderbilt University

Nuclear magnetic resonance (NMR) tomography at Nottingham: methods system technology and results

G. N. Holland, W. S. Moore, R. C. Hawkes

Department of Physics, University of Nottingham, University Park
Nottingham, NG7 2RD, United Kingdom

Abstract

The techniques employed in the Nottingham whole-body NMR imaging system are described. Attention is paid to the design philosophy of the instrument, describing in detail the construction of the apparatus. Results obtained from approximately one year's experience of head scanning are described.

Introduction

Since the first practical demonstration of nuclear magnetic resonance (NMR) imaging in 1973 by Lauterbur¹, there has been considerable research work on the subject carried out at Nottingham University. Initial experiments were performed during 1971 on a modified conventional NMR spectrometer operating at 60 MHz proton resonance frequency, using a technique devised by Moore and Hinshaw². The results obtained using this, the 'sensitive point method', were from samples up to 6 mm diameter. In 1975 a research team was set up to construct an imaging system to operate at 30 MHz with access for samples up to 8 cm diameter. This machine which became operational in 1977 was designed solely for operation using the 'multiple sensitive point' technique of Hinshaw. A wide range of images were produced using the apparatus from animal³, vegetable⁵, and mineral⁶ samples.

In 1978 two of the authors (WSM, GNH) initiated a program to construct a whole-body NMR imaging system; the aim being to produce a versatile instrument not restricted to one particular technique. This paper describes the NMR methods which have been implemented on the apparatus, and discusses in detail the design philosophy behind the construction of the equipment. The results obtained to date are also discussed.

Methods

The scaling up of an NMR system presents special problems due to the low frequency, large size and inherently low sensitivity of the experiment. Experience gained with the small 30 MHz system using the multiple sensitive point (MSP) technique indicated that even if this method was not optimal in terms of efficiency of data collection it was at least capable of producing high resolution NMR images. Consequently it was decided to implement this technique at whole-body sizes. For more rapid data collection, the ability to perform projection reconstruction methods under a wide range of pulse techniques was also included in the design schedule.

Initial results were obtained from the apparatus using the MSP technique. In this technique a unique column of spins through the sample by applying two orthogonal sinusoidally modulated field gradients. A third mutually orthogonal static field gradient is used to give a spread in resonant frequencies along the column.

The direction of a uniform field gradient is the direction along which the field changes at a maximum rate; the field in the plane perpendicular to this does not vary. In the apparatus coil systems are so arranged so as to produce magnetic fields in the z direction, which is also the direction of the steady applied magnetic field B_{z0} . The three gradient fields are therefore:-

$$\begin{aligned} g_z \cdot z \cdot \cos \Omega t \\ g_x \cdot (x - x_0) \sin \Omega t \\ g_y \cdot y \end{aligned}$$

where the gradient strength g_x , g_y and g_z are the spatial rates of change of B_z in the x, y and z directions: Thus the total field experienced at any point in an extended sample, centre (0,0,0) is:-

$$B_z(x,y,z,t) = B_{z0} + g_x(x - x_0) \sin \Omega t + g_y \cdot y + g_z \cdot z \cos \Omega t \quad (1)$$

The total field is thus time dependent with frequency of oscillation Ω everywhere except along the 'sensitive line' $x = x_0, z = 0$.

In order to collect components of signal with no time dependence, the signal is averaged over a large integral number of gradient cycles. Only time independent signals can be moved electronically by altering x_0 , the position where the x gradient contributes zero field which is achieved by varying the ratio of currents fed to the pair of currents that generates g_x . Thus a thin section image in the plane $x = 0$ can be obtained. The actual dimensions of the sensitive line depend on g_z which alters section thickness and g_x which alters resolution in the x direction.

In the MSP method, in combination with the field gradient scheme described above a pulse technique called steady-state free precession (SFP) is employed which consists of applying a rapid sequence of phase alternated resonant RF field pulses at ω_0 to the specimen. After a time $\sim T_1$ (the spin-lattice relaxation time) an equilibrium is set up where the steady-state NMR signal S can be approximated by:-

$$S \propto \frac{\rho \sin \alpha}{(T_1/T_2 + 1) - (T_1/T_2 - 1) \cos \alpha} \quad (2)$$

for a homogeneous collection of protons with longitudinal and transverse relaxation times respectively. Here ρ is the actual number density of hydrogen atoms and $\alpha = \gamma H_1 \delta$ (where γ is the gyromagnetic ratio, H_1 the RF field strength and δ RF pulse duration). The condition of maximum signal amplitude is when $\alpha = \pi/2$ (a '90° pulse') and $T_1 = T_2 \gg \tau$ where τ is the RF interpulse interval. Under these conditions signal amplitude is directly proportional to proton density. However this does not mean that the greatest degree of image contrast is exhibited at a maximum signal condition. The observed signal S' is the sum of responses S of many types of proton with differing values for the ratio T_1/T_2 . Some information about the type of proton contributing to S' can be obtained by observation of the behaviour of S' as α is varied. This is shown in Figure 1 where normalized signal amplitude is plotted against pulse angles for various $T_1:T_2$ ratios typical of those encountered in biological systems. Examination of the curves indicate that whilst signal maxima are obtained for $\alpha > 90^\circ$ the greatest discrimination between components occurs at $90^\circ < \alpha < 120^\circ$. It therefore can be seen that combinations of pulse lengths and power can be used to influence α in order to vary image contrast.

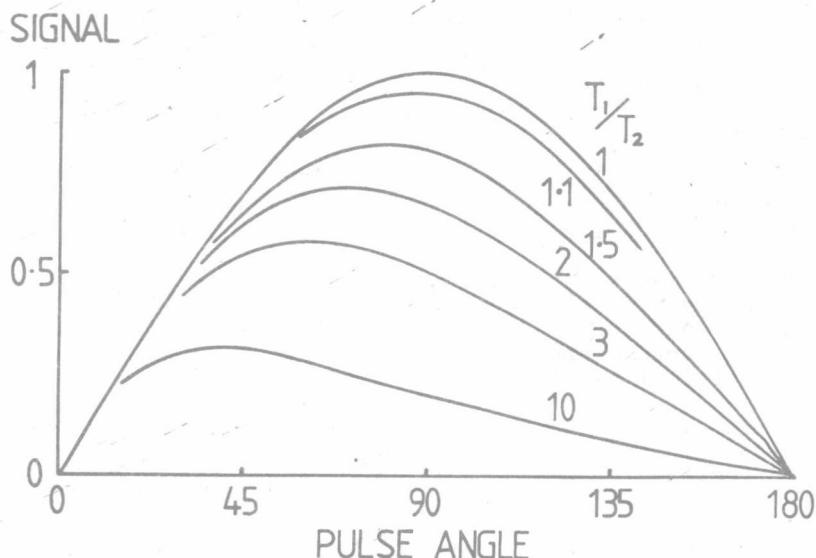


Figure 1: Signal response vs pulse angle for various $T_1:T_2$ ratios.

Facilities in the apparatus are also provided to obtain projection data for image reconstruction by filtered back projection. In this case the field gradients must be handled rather differently than for the MSP technique. Assuming transverse plane imaging g_z remains time dependent but g_x becomes a static linear gradient. During the course of an experiment g_x and g_y are generated by coil sets driven with currents of the form $I \sin \theta$ and $I \cos \theta$ where θ has a range of 0 to π , and traverses this range in a total of N steps where N is the number of projections collected. Since a field gradient is a vector it can be seen that the resultant of g_x and g_y is:-

$$g_{xy}(\cos^2\theta + \sin^2\theta)^{\frac{1}{2}} = |g_{xy}| \quad (3)$$

Any point on $|g_{xy}|$ therefore traverses an arc of 180° during the course of a scan. As in the MSP method collecting only time independent data results in a thin section image in the plane $z = 0$.

If the coils that generate g_z are separately driven, then by varying the ratio of currents in the two coil half sets the zero field plane position can be shifted, allowing a set of images of parallel planes through the specimen to be obtained without any movement of that specimen. The range through which the zero field plane may be moved is dependent on the linearity of the gradients and/or the range of receiver coil sensitivity. Furthermore, by reallocating the time dependent field gradient to either g_x or g_y with static gradient rotation in the yz or xz plane sagittal or coronal images may also be generated.

Further aspects of the methods relating to data collection and processing are discussed in the next section as they are closely related to the particular instrumentation used.

Apparatus

Magnet, Gradient and RF Coils

The primary consideration for any whole-body NMR imaging is the selection of the magnet system. At the time the authors were considering their choice of magnet only four systems of any type to their knowledge had been delivered worldwide, and all were of the 4-coil resistive air cored solenoid type. Whilst the acquisition of a superconducting magnet system was discussed this was ruled out easily on several grounds - most notably cost - but also delivery schedule and environmental specifications. Since only proton NMR imaging was envisaged the major feature of superconducting by magnet systems - namely the ability to generate high field from low power input - was not considered advantageous since the RF conductive losses exhibited by body tissue above 10 MHz give rise to an upper field limit of ~ 0.25 T for proton NMR. Of the two resistive magnet types available the model with aluminium tape wound coils rather than copper wire wound coils was preferred on the grounds of anticipated superior thermal characteristics and smaller winding errors. The magnet was manufactured by Walker Scientific Inc. (Worcester, Mass.), and is capable of generating a field of 0.1 T for a 15 kW power input. Its bore is 60 cm. The 1Ω resistance exhibited by the four coils in series allowed the unit to be driven by a 220 A Varian DC regulated power supply available in the authors' laboratory. Water cooling for both magnet and power supply was provided by a custom built closed cycle cooling system. The mechanically crude coil mounting scheme incorporated in the magnet design, coupled with the desire to site the unit in a normal laboratory environment with close proximity of large amounts of ferrous material was instrumental in the decision to attempt to attain only modest field homogeneity. In practice, using AC field plotting techniques with a small NMR probe mounted on an arm capable of axial and radial movement as well as rotation in a fixed plane enabled a homogeneity of 1 part in 10^4 over a head sized volume (10 cm radius sphere) to be attained with only a few hours shimming procedure.

The form of gradient coils used in our imaging system has already been described elsewhere⁷. Golay coils are used for the generation of gradients g_x and g_y . Golay coils used to produce a gradient in the z direction consist of four current arcs spaced by 120° on a cylinder of radius R . The separation of current arcs is $0.78 R$ and the length of an individual coil is $2.13 R$. Separation of coil centres is thus $2.91 R$.

The 60 cm magnet bore allows a patient tube of 55 cm diameter with the Golay gradient coils fixed to its exterior to be used. For the Golay coils therefore $R \approx 28$ cm. These coils are linear to within $\sim 10\%$ over region of radius $0.7 R$, and to better than 5% over $0.5 R$. Since the methods to be used do not require rapid gradient changes (i.e. pulsed gradients are not employed) the coils were wound with a large number of turns. Individual coils were wound from 2.5×1.2 mm rectangular cross section enamelled copper wire and each consists of two layers each of 34 turns with a total resistance of $\sim 1 \Omega$ or 2Ω per half set. A complete set gives a gradient of $10^{-3} \text{ T m}^{-1} \text{ A}^{-1}$. The experiment requires a gradient $G = 2\pi N/\gamma t D$ where N is the number of time data points sampled in t and D is the diameter of the object. For head imaging this translates, under typical operating conditions to $\sim 6 \times 10^{-3} \text{ T m}^{-1}$, obviously therefore requiring drivers capable of providing ~ 6 A. The gradient g_z is generated by a Helmholtz pair of coils driven in opposition and mounted between patient tube and the inner coils of the 4-coil magnet. Wire diameter and number of turns, and also coil radius is chosen so that a similar resistance is exhibited by these coils when compared to x and y gradient coil sets. Resistance is also $\sim 2 \Omega$ with each coil containing 100 turns of s.w.g. enamelled copper wire wound on a 38 cm radius former.

In our apparatus the NMR probe is of the crossed coil variety, i.e. separate transmitter and receiver coils and their associated tank circuits are provided. The major reasons for this are (i) to reduce noise pick-up in the receiver from the RF amplifier (ii) to allow different receiver coils varying size and geometry to be used without disturbing the transmitter coil and tank circuit which because of their high power handling capability are difficult to construct. The transmitter coil consists of two single turn plane ellipses crossing at right angles, and wound from 2.5 mm radius copper tube on a former of 50 cm diameter. At $f_0 = 4.3$ MHz the measured inductance is ~ 14 μ H giving a tuning capacitance value C_{of} 98 pF from $C = (4\pi^2 f_0^2 L)^{-1}$. This value of capacitance and that of an associated series element for impedance matching can be provided by using high breakdown air dielectric transmitter capacitors. It is our experience, however, that with coil voltages in excess of 12 kV peak-to-peak, generated by the RF pulse, arcing can occur within the tank circuit, even when DC breakdown figures are not exceeded. Our solution has been to oil fill the complete tank circuit rather than employ expensive vacuum capacitors since in this latter case interconnections would still be susceptible to arcing. As mentioned previously several forms of receiver coil have been used for specific experiments, but for head imaging a similar geometry to that of the transmitter coil is employed, but with the field axis orthogonal to the transmitter. As diode isolation is used, only low voltages are present in the tank circuit and no special precautions, except RF shielding, are required. The receiver tank circuit output connects directly to the input of the NMR preamplifier which is sited as close as possible to the tank circuit enclosure.

The entire magnet assembly, magnet, gradient and RF coils is enclosed in an aluminium mesh Faraday cage, to reduce RF interference. All leads entering the cage are heavily filtered. Also inside the cage is a patient handling system. In order to minimize the effect of magnet field homogeneity of structural steel work in floor and ceiling of the laboratory, the magnet has been sited on a plinth so that its axis is equidistant between the two surfaces. Consequently the patient handling system incorporates a hydraulic lift facility to allow the patient to be translated from normal bed height of 800 mm to the ~ 1500 mm required for entry of the bed into the patient tube. When positioned for head scanning the patient is in visual contact with the operator by a 'periscope'. However, since no ionizing radiation is employed, it is possible for medical staff to remain with the patient inside the cage during the scanning procedure.

The Electronics

The electronics may be divided into three areas - namely high frequency analog (RF), low frequency analog and digital (control and processing).

Commencing with a description of the RF electronics which comprises the NMR spectrometer and the RF amplifier. The initial source of RF is a digitally programmable frequency synthesizer. The RF output of this unit feeds both transmitter and receiver. In the transmitter the CW RF enters phase shifters to produce phase shifts of between $\pi/4$ and $3\pi/4$. A gating network allows selection of any of the derived phases. Then follows a scheme for generating the resonant RF frequency f_0 only during the RF pulse envelope which arrives from the digital control circuitry. The resultant pulse at f_0 is fed to the RF amplifier. The RF amplifier is entirely solid state and since its recent uprating is capable of a peak pulse output of 7.5-8 kW depending on operating frequency. The basic design has been described elsewhere⁸, but basically consists of eight identical water cooled power modules, each capable of providing 1 kW into 50 Ω . The eight outputs are combined with commercial passive power couplers to derive the final output. The reason for such high power requirement can easily be seen as the power requirement to give a 900 pulse in a pulsed NMR experiment can be defined as:

$$P \approx \frac{VN^3\pi^2}{9\gamma^2\tau^3}$$

where V is the transmitter coil volume, N is the number of points sampled in interval τ . Under realistic operating conditions for a 50 cm diameter saddle shaped transmitter coil with $N > 100$ and $\tau < 10$ ms then power up to 8 kW can easily be required.

The receiver employed in the NMR system is quite conventional. The signal received from the preamplifier is further amplified and is sent eventually to a pair of phase sensitive detectors (PSD's) with references derived from synthesizer output in phase quadrature. The PSD outputs are filtered, amplified and sent to a pair of analog-to-digital converters (ADC's). The signals are sampled N times during the interval between successive RF pulses. The capability exists for up to 1 MHz throughput rate for data conversion. The ADC outputs, suitable buffered, are sent as a single 16-bit parallel data word to the processing section of the digital electronics.